

Approximation of the Bistatic Slant Range Using Chebyshev Polynomials

Carmine Clemente, *Student Member, IEEE*, and John J. Soraghan, *Senior Member, IEEE*

Abstract—The effectiveness of frequency domain processing algorithms in bistatic synthetic aperture radar (SAR) focusing depends critically on the accuracy of the bistatic slant range function approximation. This letter presents a new Chebyshev slant range function approximation that is shown to increase the accuracy of the analytical approximation of the bistatic point target spectrum. The performance of the new method is compared to the conventional Taylor series approximation approach in the generation of the point target spectrum. The new approach is shown to provide a more accurate approximation of the slant range function with negligible increase in processing requirements compared to the traditional Taylor series approximation. The accuracy improvement is shown to yield a more accurate spectrum that can be exploited in bistatic SAR focusing algorithms.

Index Terms—Bistatic synthetic aperture radar, Chebyshev approximation, point target spectrum, slant range approximation.

I. INTRODUCTION

BISTATIC synthetic aperture radar (SAR) operates with a separate transmitter and receiver introducing new characteristics compared to traditional monostatic SAR systems [1]. Some of the advantages of the bistatic configuration include the following: 1) the reduction of vulnerability of the system in military applications with the ability of having the transmitter located at safe distances from a hostile area; 2) the capability for the bistatic system to be employed for imaging in the flight direction or backward in flight assistance systems; 3) the reduction of costs; 4) the measurement of the bistatic clutter characteristic; and 5) the reduction of the dihedral and polyhedral effects in urban areas improving the image quality. However, the bistatic flight configuration poses two critical technological challenges. The first involves the synchronization of the transmitter and the receiver both in space and time. Good solutions for this issue were developed in [2] and [3].

The second critical challenge of the bistatic SAR configuration is the requirement for slant range function approximation which is significantly different from the monostatic case. The bistatic slant range function is characterized by the sum of two hyperbolas [1] rather than a single hyperbola in the monostatic case. This double squared root function makes the derivation

of a signal spectrum model for focusing algorithms in the frequency domain much more challenging than in the monostatic case. Different approaches have been proposed to address this problem, some numerical like Numeric SAR (NuSAR) [4] and the dip move out technique [5] and some mathematical such as Loffeld's bistatic formula [6] and the method of series reversion [7], [8].

In this letter, we present a new approach to the approximation of the slant range function using Chebyshev polynomials [9] in order to obtain a polynomial representation that can be used in the method of series reversion [7], [8] to obtain a more accurate version of the point target spectrum. The proposed approach replaces the coefficients of the polynomial Taylor series expansion of the bistatic slant range function with the ones obtained using the Chebyshev polynomial approximation. The obtained coefficients are then used to obtain an analytical formulation of the bistatic point target spectrum as in [7] and [8].

Compared to the Legendre approximation, proposed in [10], the Chebyshev polynomials allow us to obtain a least squares approximation of the slant range function that includes the property of a bounded maximum error, thus minimizing the so-called *Runge effect* [9]. In addition, the mathematical and computational complexity is reduced.

The remainder of this letter is organized as follows. In Section II, the bistatic SAR geometry and the signal model are discussed. In Section III, the Chebyshev polynomial approximation is introduced, while in Section IV, the new method of using Chebyshev polynomials to approximate the slant range function is developed. Section V presents comparative results that indicate the superior performance obtained to those obtained using the conventional approximation method [7], [8].

II. BISTATIC SAR GEOMETRY AND SIGNAL MODEL

In a bistatic SAR, the transmitter and the receiver can have different velocities, altitudes, and flight paths, leading to the possibility of having different acquisition configurations. The simplest case is when both transmitter and receiver have the same velocity and parallel flight paths, while a more complicated configuration exists when the platforms have different velocities and nonparallel flight paths. Fig. 1 illustrates an example of a bistatic configuration that comprises a separate transmitter and receiver where it is assumed that the transmitter and receiver platforms have different trajectories and velocities.

As in the monostatic case [11], the area to be imaged is a collection of point scatterers. This implies that it is sufficient to analyze the scene using the response of an arbitrary point scatterer and then consider the superposition of the echoes to obtain the focused image. Under the assumption that the

Manuscript received February 16, 2011; revised June 23, 2011, September 29, 2011, and November 30, 2011; accepted November 30, 2011. Date of publication January 18, 2012; date of current version May 7, 2012. This work was supported in part by the Engineering and Physical Research Council (Grant N. EP/H012877/1), by the MOD University Defence Research Centre in Signal Processing, and by Selex-Galileo Edinburgh.

The authors are with the Centre for Excellence in Signal and Image Processing, Department of Electronic and Electrical Engineering, University of Strathclyde, G1 1WX Glasgow, U.K. (e-mail: carmine.clemente@eee.strath.ac.uk; j.soraghan@eee.strath.ac.uk).

Digital Object Identifier 10.1109/LGRS.2011.2178812

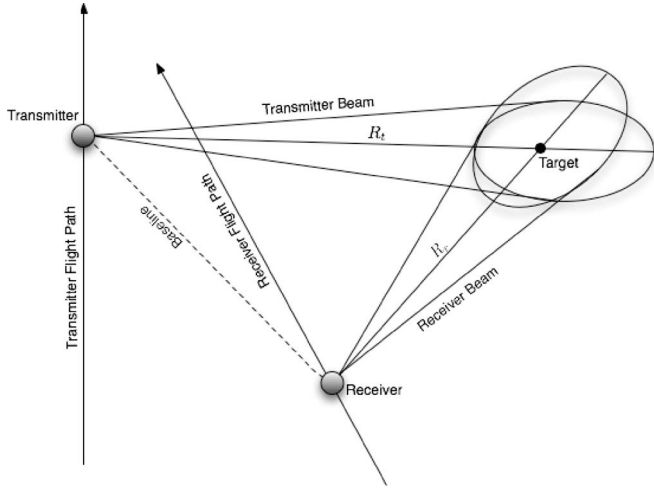


Fig. 1. Acquisition geometry for bistatic SAR.

platforms generally fly with constant velocities and in a linear path, the instantaneous slant range $R(\eta)$ may be written as

$$R(\eta) = \sqrt{V_T^2 \eta^2 + R_{Tcen}^2 - 2V_T \eta R_{Tcen} \sin \theta_{sqT}} + \sqrt{V_R^2 \eta^2 + R_{Rcen}^2 - 2V_R \eta R_{Rcen} \sin \theta_{sqR}} \quad (1)$$

where η is the slow (along track) time, V_T and V_R are the velocities, R_{Tcen} and R_{Rcen} are the range distances for $\eta = 0$, and θ_{sqT} and θ_{sqR} are the squint angles for the transmitter and the receiver, respectively. Equation (1) converts to the monostatic case when the velocities, positions, and flight paths for both the platforms are identical.

The monostatic and bistatic slant range functions for five point scatterers with the same range but different azimuth positions are shown in Fig. 2(a) and (b), respectively. The parameters of the simulated configurations are shown in Table I. In Fig. 2(a), the hyperbolic shape of the monostatic slant range function can be clearly seen, and in Fig. 2(b), the slant range function of the bistatic case is no longer a hyperbola. Instead, it is a flat-top hyperbola which changes in shape depending on the position of the scatterer. The minimum of this slant range function is related to the point of stationary phase; hence, the stationary points change with the slant range.

In the case of a transmitted linear frequency-modulated chirp signal, the received bistatic signal model can be written as

$$s(\tau, \eta) = A_0 w_r \left(\tau - \frac{R(\eta)}{c} \right) w_{az}(\eta) \times \exp \left\{ -j \frac{2\pi f_0 R(\eta)}{c} + j\pi K_r \left[\tau - \frac{R(\eta)}{c} \right]^2 \right\} \quad (2)$$

where τ is the fast time, A_0 is the complex backscatterer coefficient, f_0 is the carrier frequency, K_r is the range chirp rate, $w_r(\cdot)$ is the range envelope, and $w_{az}(\cdot)$ is the composite antenna pattern of the transmitter and receiver. The only differences between the expression of the signal model in the bistatic and the monostatic case are the slant range function and the composite antenna footprint.

The double square root shape of the slant range function in the bistatic case makes it more difficult to form a mathematical representation of the signal model spectrum that is required in order to derive focusing algorithms in the frequency domain [6].

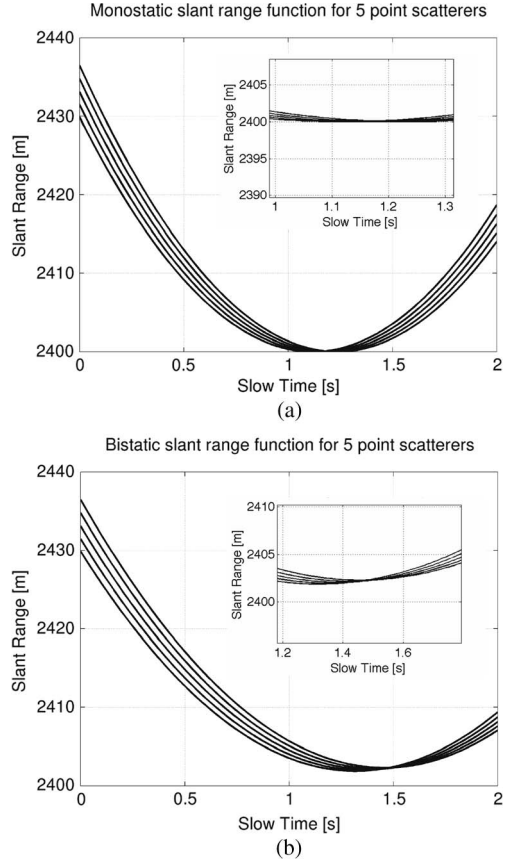


Fig. 2. Slant range for different point scatterers for the monostatic and the bistatic case. (a) Monostatic case. (b) Bistatic case.

TABLE I
MONOSTATIC AND BISTATIC SIMULATED CONFIGURATIONS.
NOTE: FOR THE MONOSTATIC CASE, ONLY THE
TX PARAMETERS MUST BE CONSIDERED

<i>Tx Velocity</i>	170 m/s
<i>Rx Velocity</i>	100 m/s
<i>Range distance of the Tx from the scene centre at $\eta = 0$</i>	1400 m
<i>Range distance of the Rx from the scene centre at $\eta = 0$</i>	1100 m
<i>Transmitter Squint angle</i>	3 deg
<i>Receiver Squint angle</i>	2 deg

III. POLYNOMIAL APPROXIMATIONS USING CHEBYSHEV POLYNOMIALS

The Weierstrass theorem [12] suggests that polynomial approximation of a continuous function in an interval $[a, b]$ can be always performed.

A common approach in obtaining an approximating polynomial is to minimize the square residual for the approximation of a function.

This minimization finds a solution for the least squares problem, which is solved using an interpolating polynomial family of orthogonal polynomials. The use of this kind of polynomial approximation facilitates convergence to the target function as the approximation order increases.

The orthogonal Chebyshev polynomials allow us to obtain an approximation which minimizes the error in the sense of the least squares [12] and the infinity norm. Another property is to reduce the so-called Runge phenomenon, meaning that the maximum approximation error is bounded.

In general, the Chebyshev polynomial approximation offers closer approximation to the minimax polynomial which represents the polynomial with the smallest maximum deviation from the true function [13], [14]. It was shown that the use of Chebyshev polynomials to approximate functions outperforms the Taylor series expansion. For these reasons, the Chebyshev approximation was chosen in this work to replace the Taylor series in the slant range function approximation used in [7] and [8]. The properties of the Chebyshev polynomial approximation lead to a better approximation of the phase history of the signal allowing the design of a more accurate matched filter to improve the image quality, and this result is achieved by the reduction of the overall error and by the reduction of the Runge effect approximating better the slant range function at the start and at the end of the acquisition.

IV. SLANT RANGE APPROXIMATION

In this section, the Chebyshev approximation is used to represent the double squared root range function of the bistatic SAR geometry shown in Fig. 1. The Chebyshev approximation is stopped at the fourth order for the computation of $R(\eta)$. In this way, our analysis is comparable with that in [7] and [8] in order to show that using the Chebyshev polynomial, with the same order of the expansion, results in better approximation of the slant range function. In addition, the uncompensated phase error should be limited to be within $\pm\pi/4$, in order to keep good image quality, and the fourth-order approximation can guarantee this condition for a large family of acquisition configurations for the approach used in [7] and [8]. The order can be reduced to the third in the cases where the phase error is already within the limits of $\pm\pi/4$, while if the specific application would require a higher phase accuracy, the order of the approximation can be increased. We will demonstrate that our approach leads to a better accuracy also in terms of phase accuracy at parity of order of the approximation.

The resulting polynomial approximation of $R(\eta)$ is

$$\begin{aligned}\hat{R}_{Cheb}(\eta) &= \sum_{k=0}^n c_k T_k(\eta) \\ &= c_0 + c_1 T_1(\eta) + c_2 T_2(\eta) + c_3 T_3(\eta) + c_4 T_4(\eta) \\ &= 8c_4 \eta^4 + 4c_3 \eta^3 + \eta^2(2c_2 - 8c_4) + \eta(c_1 - 3c_3) \\ &\quad + c_0 - c_2 + c_4\end{aligned}\quad (3)$$

where T_i denotes the Chebyshev polynomials of the first kind and c_i denotes the Chebyshev coefficients computed on the Chebyshev nodes [9]. There are four kinds of Chebyshev polynomials, and the first kind is used in this letter. However, all the four kinds of Chebyshev polynomials share the same properties and could be used with similar quality of the approximation [13].

The coefficients in (3) can be grouped as follows:

$$\begin{aligned}g_0 &= c_0 - c_2 + c_4 & g_1 &= c_1 - 3c_3 \\ g_2 &= 2c_2 - 8c_4 & g_3 &= 4c_3 & g_4 &= 8c_4.\end{aligned}\quad (4)$$

Now, (3) can be written as

$$\hat{R}(\eta)_{Cheb} = g_4 \eta^4 + g_3 \eta^3 + g_2 \eta^2 + g_1 \eta + g_0. \quad (5)$$

Equation (5) is the Chebyshev approximation in polynomial form of the bistatic slant range function. The fundamental difference between this new approximation in (5) to that reported in [7] and [8] is that the coefficients for the spectrum are now computed starting from the coefficients g_i , which are obtained with the Chebyshev approximation rather than the Taylor approximation.

The 2-D point target spectrum [7], [8] is derived using the formulation in (5). Starting from the Fourier transform of the range compressed signal, in order to obtain the 2-D point target spectrum, the principle of stationary phase is applied. In this, the approximated version of the slant range function replaces the phase term of the azimuth Fourier transform. This yields a power series expression that links the slow time with the Doppler frequency. Inverting the power series using the method of series reversion produces the desired 2-D point target spectrum. The resulting 2-D point target spectrum is

$$S_{2df}(f_\tau, f_\eta) = W_r(f_\tau) W_{az} \left(f_\eta + (f_0 + f_\tau) \frac{g_1}{c} \right) \times \exp j \Phi_{2df}(f_\tau, f_\eta) \quad (6)$$

where

$$\begin{aligned}\Phi_{2df}(f_\tau, f_\eta) &\approx -2\pi \left(\frac{f_0 + f_\tau}{c} \right) g_0 \\ &\quad + 2\pi \frac{c}{4g_2(f_0 + f_\tau)} \left(f_\eta + (f_0 + f_\tau) \frac{g_1}{c} \right)^2 \\ &\quad + 2\pi \frac{c^2 g_3}{8g_2^3 (f_0 + f_\tau)^2} \left(f_\eta + (f_0 + f_\tau) \frac{g_1}{c} \right)^3 \\ &\quad + 2\pi \frac{c^3 (9g_2^3 - 4g_2 g_4)}{64g_2^5 (f_0 + f_\tau)^3} \left(f_\eta + (f_0 + f_\tau) \frac{g_1}{c} \right)^4\end{aligned}\quad (7)$$

and g_i , $i = 0, 2, \dots, 4$, denotes the coefficients of the Chebyshev polynomial approximation given in (4).

In the proposed approach, the computational cost to compute the coefficients g_i is reduced to the evaluation of the slant range function in the Chebyshev nodes and a sum over n real value multiplication values, where n is the approximation order. The computation of the coefficients in the Taylor-based approach is stopped at the fourth order. This requires the evaluation of 4 trigonometric functions, 2 square roots, and about 60 multiplications, while for the Chebyshev approach, the required computations are 8 square roots and about 60 multiplications. For this reason, the computational costs of both approaches are comparable. If the order of the approximation is increased, the Taylor-based approach increases its complexity more than the Chebyshev approach. This is due to the higher number of terms required in the computation of the coefficients. Furthermore, considering the computational burden required in the entire image formation process that includes all the fast Fourier transforms, matched filters, chirp scaling or range cell migration correction, autofocus, etc., then the time required to approximate the range history is negligible.

V. RESULTS

Azimuth-invariant and azimuth-variant configurations are characterized by a fixed and varying baseline between the transmitter and the receiver, respectively. Generally, it is difficult to keep the configuration azimuth invariant, and the case

TABLE II
BISTATIC SIMULATION PARAMETERS

	Azimuth invariant	Azimuth variant
Carrier Frequency	5 GHz	5 GHz
PRF	1000 Hz	1000 Hz
Tx Velocity	90 m/s	100 m/s
Rx Velocity	90 m/s	70 m/s
Range distance of the Tx at $\eta = 0$	15000 m	15000 m
Range distance of the Rx at $\eta = 0$	14500 m	14500 m
Azimuth distance of the Tx at $\eta = 0$	45 m	45 m
Azimuth distance of the Rx at $\eta = 0$	80 m	80 m
Pulse duration	6 μ s	6 μ s
Range Bandwidth	50 MHz	50 MHz

TABLE III
MEASURED SLL, PSLR, AND ISLR VALUES
FOR THE AZIMUTH-INVARIANT CASE

	SLL [dBs]	PSLR [dBs]	ISLR [dBs]
Taylor-Range Gate	-14.14	-16.54	-10.99
Chebyshev-Range Gate	-14.26	-16.72	-11.10
Taylor-Azimuth Gate	-13.52	-16.03	-10.30
Chebyshev-Azimuth Gate	-13.60	-16.05	-10.40

of azimuth-variant configurations is the most frequent. In the performance analysis, both configurations were simulated. In the first test (azimuth invariant), a point scatterer in the center of the scene (azimuth sample = 1000 and range sample = 182) is simulated. From the 2-D spectrum of the range compressed received signal, the value of $\Phi_{2df}(f_\tau, f_\eta)$ is compensated, obtaining the point target response of the bistatic SAR system. The improvement in the quality using the Chebyshev approach is measured using the sidelobe level (SLL), the peak sidelobe ratio (PSLR), and the integrated sidelobe ratio (ISLR). The SLL is defined as the level of the first sidelobe while the PSLR and the ISLR are defined as follows:

$$PSLR = 10 \log \frac{\text{maximum sidelobe power}}{\text{main lobe power}}$$

$$ISLR = 10 \log \frac{\text{total power in sidelobes}}{\text{main lobe power}}$$

The results shown in Table III are obtained measuring the impulse response in the case of a bistatic azimuth-invariant configuration with parameters given reported in Table II using the Taylor and Chebyshev coefficients for the 2-D phase of the point target spectrum.

The results for the range and azimuth gates using the two approaches are shown in Table III. These results show that the proposed approach allows us to obtain an improvement in the bulk compression in terms of power in the sidelobes. This result is due to the more accurate approximation of the slant range function with the Chebyshev approach leading to a more accurate analytical solution of the point target spectrum.

A second simulation is performed using the bistatic azimuth-variant configuration as specified in Table II. The first result in Fig. 3 shows the approximation of the slant range function using the Taylor and the Chebyshev polynomial. The maximum error is of 0.06 m, while using the Chebyshev approximation, the maximum error is 3.63×10^{-11} m. These results indicate that the polynomial coefficients obtained with the Chebyshev approach improve the accuracy of the approximation. This result has a direct impact on the accuracy of the point target spectrum. Fig. 4 shows the phase error of the point target spectrum using the Taylor and the Chebyshev approximation

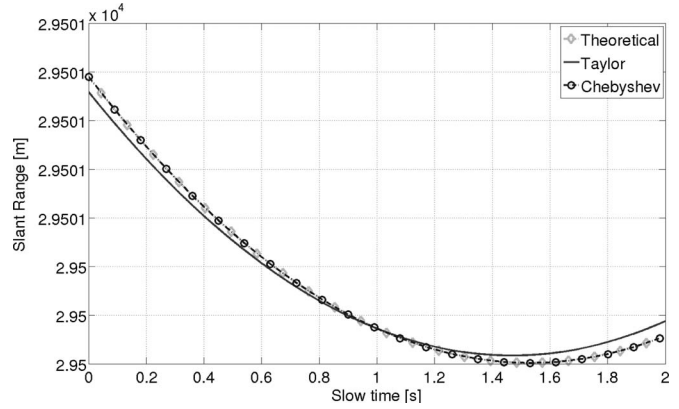


Fig. 3. Approximations of the slant range function using Taylor and Chebyshev approximation.

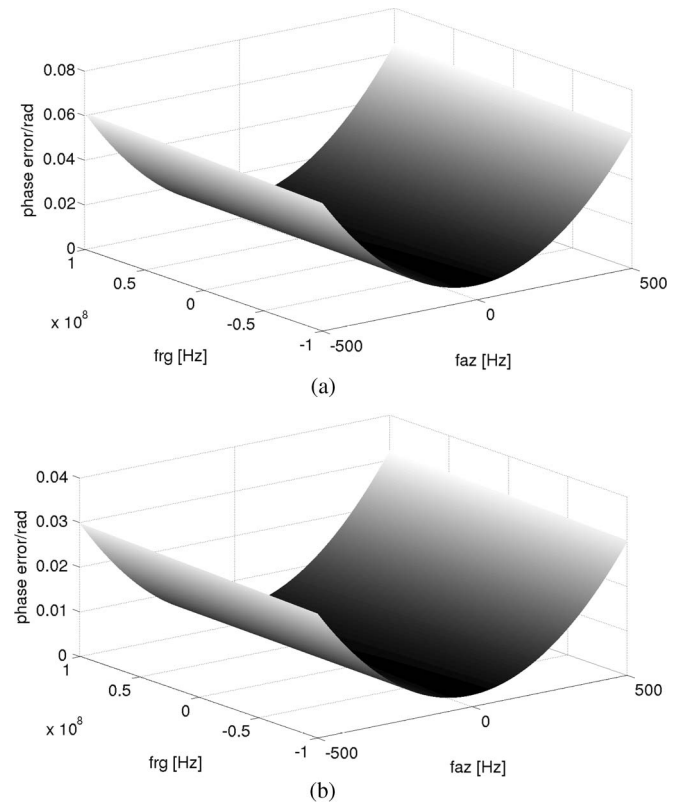


Fig. 4. Phase error for the azimuth-variant configuration reported in Table II. (a) Taylor approximation. (b) Chebyshev approximation.

TABLE IV
MEASURED SLL, PSLR, AND ISLR VALUES
FOR THE AZIMUTH-VARIANT CASE

	SLL [dBs]	PSLR [dBs]	ISLR [dBs]
Taylor-Range Gate	-12.30	-15.40	-10.21
Chebyshev-Range Gate	-14.32	-18.04	-12.33
Taylor-Azimuth Gate	-13.01	-15.31	-9.52
Chebyshev-Azimuth Gate	-13.42	-15.49	-10.12

for the bistatic configuration in Table II. The configuration exhibits a moderate squint angle, and the phase error is seen to be reduced by the use of the Chebyshev approximation. This implies that the Chebyshev-based approach is more robust, thus facilitating the processing of a wider family of bistatic configurations. The results for the respective impulse responses obtained using this configuration are reported in Table IV.

TABLE V
MEASURED MAXIMUM ERROR FOR APPROXIMATION
ORDER FROM 1 TO 6

Order	Max Error Taylor [m]	Max Error Chebyshev [m]
1	0.564	0.251
2	0.062	$2.97e^{-6}$
3	0.062	$5.859e^{-7}$
4	0.062	$3.638e^{-11}$
5	0.062	$4.786e^{-7}$
6	0.062	$4.786e^{-7}$

TABLE VI
MEASURED STANDARD DEVIATION (σ) OF THE ERROR
FOR APPROXIMATION ORDER FROM 1 TO 6

Order	σ Error Taylor [m]	σ Error Chebyshev [m]
1	0.154	0.077
2	0.017	$7.900e^{-7}$
3	0.017	$1.806e^{-7}$
4	0.017	$7.790e^{-12}$
5	0.017	$1.474e^{-7}$
6	0.017	$1.474e^{-7}$

In this case, the advantage in using the new Chebyshev approximation method approach is more pronounced compared to the azimuth-invariant case. In particular, in the azimuth direction, the power in the main lobe is observed to be significantly increased when using the Chebyshev approximation. This confirms the capability of the new method in handling shape variations of the slant range function, which are more evident in the azimuth-variant configuration.

By increasing the order of the approximation, a problem of numerical instability can appear. This is due to the fact that the coefficients of the Chebyshev series become very small. This aspect has also been analyzed through simulations by comparing the performances of the Taylor and the Chebyshev approximation for different approximation orders. The results of the measured approximation error obtained using the parameters in Table II are reported in Table V and Table VI: From these results, it is evident that increasing the order of the Chebyshev approximation reduces the capability to outperform the Taylor series approximation, and this aspect is in contrast with the theoretical analysis because of the numerical instability. However, the results are still much better than the Taylor series approximation.

VI. CONCLUSION

In this letter, a new polynomial Chebyshev approximation of the bistatic slant range function was analytically derived. The proposed approximation is intended to replace the Taylor approximation of the slant range function used in [7] and [8] to derive the analytical bistatic point target spectrum. The proposed approximation is easy to compute and does not increase the computational complexity with respect to the Taylor-based approach.

The use of the Chebyshev polynomials leads to a least squares approximation (minimizing the L^2 norm of the error),

in addition to obtaining a bound on the maximum error (minimizing the L^∞ norm of the error). This means that the approximated phase history will be closer to the original, allowing a more accurate focusing stage.

The approximation errors using the Taylor and the Chebyshev polynomials have been evaluated in this work, confirming the theoretical capability of the Chebyshev approach to minimize the norm of the error. However, working with such an accurate approximation some numerical instability may occur, and this aspect must be considered in the choice of the approximation order.

The new Chebyshev polynomial coefficients have been used to replace the Taylor coefficients in the analytical bistatic point target spectrum. The resulting point target spectrum has been tested with an azimuth-invariant and an azimuth-variant bistatic configuration. The results confirm that the Chebyshev approximation provides a more accurate approximation of the bistatic point target spectrum, leading to a more accurate and correctly located impulse response.

ACKNOWLEDGMENT

The authors would like to thank the anonymous reviewers for their useful comments and suggestions.

REFERENCES

- [1] M. Cherniakov, *Bistatic Radar: Emerging Technology*. Hoboken, NJ: Wiley, 2008.
- [2] C. Gierull, C. Pike, and F. Paquet, "Mitigation of phase noise in bistatic SAR systems with extremely large synthetic apertures," in *Proc. EUSAR*, Dresden, Germany, 2006.
- [3] G. Krieger and Y. Marwan, "Impact of oscillator noise in bistatic and multistatic SAR," *IEEE Geosci. Remote Sens. Lett.*, vol. 3, no. 3, pp. 424–429, Jul. 2006.
- [4] R. Bamler and E. Boerner, "On the use of numerically computed transfer functions for processing of data from bistatic SARs and high squint orbital SARs," in *Proc. IEEE IGARSS*, Jul. 2005, vol. 2, pp. 1051–1055.
- [5] D. D'Aria, A. Guarnieri, and F. Rocca, "Focusing bistatic synthetic aperture radar using dip move out," *IEEE Trans. Geosci. Remote Sens.*, vol. 42, no. 7, pp. 1362–1376, Jul. 2004.
- [6] O. Loffeld, H. Nies, V. Peters, and S. Knedlik, "Models and useful relations for bistatic SAR processing," in *Proc. IEEE IGARSS*, Jul. 2003, vol. 3, pp. 1442–1445.
- [7] Y. L. Neo, "Digital processing algorithms for bistatic synthetic aperture radar data," Ph.D. dissertation, Univ. British Columbia, Vancouver, BC, Canada, 2007.
- [8] Y. L. Neo, F. Wong, and I. Cumming, "A two-dimensional spectrum for bistatic SAR processing using series reversion," *IEEE Geosci. Remote Sens. Lett.*, vol. 4, no. 1, pp. 93–96, Jan. 2007.
- [9] J. Mason, *Chebyshev Polynomial: Theory and Applications*. Norwell, MA: Kluwer, 1996.
- [10] F. Wang and X. Li, "A new method of deriving spectrum for bistatic SAR processing," *IEEE Geosci. Remote Sens. Lett.*, vol. 7, no. 3, pp. 483–486, Jul. 2010.
- [11] I. Cumming and F. Wong, *Digital Processing of Synthetic Aperture Radar Data: Algorithms and Implementation*, 1st ed. Norwood, MA: Artech House, 2005.
- [12] T. J. Rivlin, *An Introduction to the Approximation of Functions*. New York: Dover, 2003.
- [13] J. Mason (1993, Dec.). Chebyshev polynomials of the second, third and fourth kinds in approximation, indefinite integration, and integral transforms. *J. Comput. Appl. Math.* [Online]. 49(1–3), pp. 169–178. Available: <http://www.sciencedirect.com/science/article/pii/0377042793901485>
- [14] M. Abutheraa and D. Lester, "Computable function representation using effective Chebyshev polynomial," in *Proc 4th CMSE*, 2007, pp. 103–109.